

# Effects of Soda Lime Silica Glass Content on the Dielectric Properties of Polytetrafluoroethylene Matrix at Microwave Frequencies

<sup>1</sup>Ibrahim Abubakar Alhaji, <sup>2</sup>Zulkifly Abbas & <sup>1</sup>Abdullahi Muhammad

<sup>1</sup>Department of Physics, Federal University of Kashere, P.M.B. 0182 Gombe, Gombe State, Nigeria

<sup>2</sup>Department of Electrical and Electronics Engineering, Xiamen University Malaysia, 43900 Sepang, Selangor Darul Ehsan, Malaysia

✉: alhaji259@gmail.com; +2348084998581

Received: 16.12.2023

Revised: 25.05.2024

Accepted: 04.06.2024

Published: 06.06.2024

## Abstract:

Polytetrafluoroethylene (PTFE)-based composites are widely in demand for microwave substrate application due to their excellent dielectric properties and low power loss. In this work, PTFE matrix filled with different contents (5 wt.% – 25 wt.%) of soda lime silica (SLS) glass powder were prepared and fabricated via dry powder processing technique. The SLS glass powder was acquired through milling process. X-ray diffraction (XRD) was used to characterise the composites for phase identification. In addition, dielectric properties of the composites were measured using open-ended coaxial probe (OCP) technique at 1 GHz to 12 GHz microwave frequencies. The XRD pattern of the composites confirmed the phase of PTFE and highlighted the interaction between the PTFE and SLS phases. The results, also, revealed that relative permittivity ( $\epsilon'$ ) and loss tangent ( $\tan\delta$ ) decrease with frequency, while they appreciate with the SLS filler content. Furthermore, the composites exhibited optimum dielectric properties at 10 GHz for 10 wt.% SLS filler with  $\epsilon'$  and  $\tan\delta$  values of 2.23 and 0.0011, respectively. This result was favourably compared with some reported PTFE-based composites characterised using other methods, thereby, indicating the suitability of OCP technique for characterising solid dielectric materials for microwave substrate application.

**Keywords:** Loss tangent, Microwave, OCP, PTFE, Relative permittivity

## 1. Introduction

The advent of microwave (microelectronics) devices for high data throughput for civil and defence electronic applications demands for efficient microwave substrates for fast high-data transmission [1,2]. It is a requirement for microwave substrate to have low relative permittivity or dielectric constant ( $\epsilon'$ ), loss factor ( $\epsilon''$ ), and loss tangent ( $\tan\delta$ ). The  $\tan\delta$  being a ratio of the  $\epsilon''$  to the  $\epsilon'$ . The low value of  $\epsilon'$  ensures fast signal transmission across the substrate with little or no delay, while low  $\tan\delta$  results in minimal signal power loss. Thus, accurate dielectric characterisation of the composites is critical to the development of substrate materials with suitable dielectric properties for microwave application. Polymer-based composites are normally used for high frequency substrates [3]. However, polytetrafluoroethylene (PTFE)-based composites were more popular due to their low dielectric properties. Because PTFE has the lowest dielectric properties among the

polymers ( $\epsilon' = 2.1$  and  $\tan\delta = 10^{-4}$ ), which are steady over a large frequency range [4–8].

Several methods of characterising the dielectric properties of PTFE-based composites have been employed, such as resonance method [4], Hakki-Coleman method [7,9], waveguide cavity perturbation technique [10]. Although, these methods were accurate, however, a simpler and easier technique to implement, such as open-ended coaxial probe (OCP) technique [11] can be employed for the characterisation of the dielectric composites. The OCP technique is mainly developed to characterise liquid and semi-solid materials [12]. Several studies have utilised the technique for dielectric characterisation [13–16]. The technique is a one-port measurement system connected to the vector network analyser comprising a truncated line with a sensor probe attached as a point of contact with a device under test (DUT). The sensor detects the reflected signal from the DUT. For the accuracy of the measurement, a good contact should be established between the probe and sample by smoothing and flattening the sample's surface. The main advantage of the technique lies in its capacity

for broadband capabilities, simple measurement procedure and less demanding sample preparation [17,18].

Although, the application of OCP technique has been utilised for dielectric samples, there were few works of literature on its usage for characterising PTFE-based composites at microwave frequencies. Thus, this work fabricates and characterises PTFE/SLS composites using the OCP technique. The characterisation will be conducted at microwave frequency range of 1 GHz to 12 GHz at room temperature. Furthermore, the work studies the impact of SLS filler loading on the PTFE/SLS composites for microwave substrate application.

## 2. Materials and Method

This section discussed the materials used and the method employed for this research work.

### 2.1 Materials

PTFE supplied by Fujian Sannong New Materials Co., Ltd, China and waste SLS glass bottles were used as the initial materials to prepare the PTFE/SLS composites. The glass bottles were sourced from a recycling site at Serdang, Selangor, Malaysia.

### 2.2 Fabrication of PTFE/SLS Composites

The SLS glass bottles were cleansed and broken into pieces before being loaded into a mill jar for milling. The mill jar was loaded with a powder-to-ball ratio of 20:1 for crushing the bottle pieces into a powdery form. Also, the milling was conducted at 45 rpm for 24 hr via a U.S. Stoneware Jar Mills (U.S. Stoneware, East Palestine, Ohio, USA). After the milling, the powder was sieved to 63  $\mu\text{m}$  particle grain size and mixed with PTFE using a high-speed dry mixer for 10 min. The mass percentage of the SLS powder was varied from 5 wt. % - 25 wt.% of the total volume of each composite. After that, all samples were pressed using a hydraulic press at 10 MPa for 5 min. Finally, the compact samples were sintered to remove particles coalescence and voids [19]. The sintering process is as shown in Figure 1.

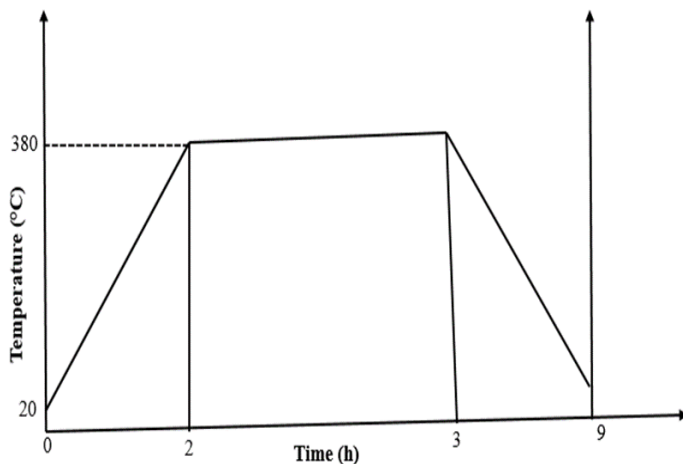


Fig. 1. Sintering process

### 2.3 Characterisation

The characterisation techniques being adopted were highlighted in this section.

#### 2.3.1 X-Ray Diffraction

X-ray diffraction (XRD) is a non-destructive technique used to determine the crystal structure, lattice parameters and the spacing between lattice planes of semi-crystalline and crystalline materials. In this work, the XRD technique was employed to analyse the structure and phase composition of PTFE/SLS composites. The XRD data were gathered using a computerised Philips X'pert system (Model PW3040/60 MPD) with Cu-K $\alpha$  radiation functional at a voltage of 40.0 kV and a current of 40.0 mA. Also, a scanning speed of 2.0° per min was used at a wavelength of 1.5405 Å. In addition, a 10–70° 2-theta range was used to record the diffraction pattern of the samples. All data were evaluated in the Rietveld analysis on X'Pert Highscore Plus v3.0 software (PANalytical B. V., Almelo, The Netherlands). The powders were identified by comparing their diffraction peaks with the Inorganic Crystal Structure Database (ICSD).

#### 2.3.2 Complex Permittivity

PTFE/SLS composites were investigated for the  $\epsilon'$  and  $\epsilon''$  [20] in the 1 – 12 GHz microwave frequency domain. The investigation was conducted at room temperature. The  $\epsilon'$  and  $\epsilon''$  represent energy storage and loss of the dielectric material. In addition, a ratio of  $\epsilon'$  and  $\epsilon''$  was computed to get the loss tangent ( $\tan\delta = \epsilon''/\epsilon'$ ) of individual composites [21,22]. Furthermore, an open-ended coaxial probe (OCP) technique was used for the characterisation [16]. The probe was connected to an Agilent N5230A PNA-L Vector Network Analyser (Agilent Technologies, Santa Clara, CA, USA). In addition, a one-port reflection calibration technique was utilised. After that, a standard PTFE material was characterised to verify the accuracy of the calibration. Data were taken by placing the OCP probe on the even and flat surface of the samples. Also, air gaps between the contact surfaces of the probe and composites likely to affect the measurement were avoided. The dimension of all composites fabricated was 6 cm x 3.6 cm x 0.7 cm.

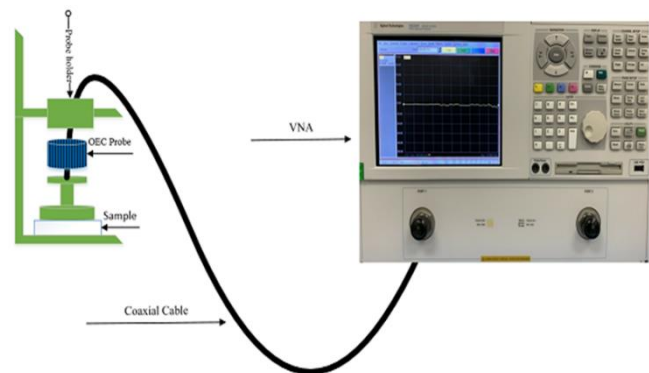


Fig. 2. OCP Measurement Set-up

#### 2.3.3 Signal Speed

Substrate materials become integral part of microwave circuitry at high frequencies. Their properties determines the dimension

of the circuit, thus, the characteristics of microwave circuits and devices being developed[19]. Similarly, because of the requirement of transmitting volume of data at high speed, substrate materials with low relative permittivity (dielectric constant) are needed to avoid unnecessary signal propagation delay. Thus, examining the influence of filler content on the propagation speed is crucial to the design and fabrication of the high frequency circuitry for super-fast data transmission. Thus, the propagation speed,  $V_s$ , can be determined using equation 1 as discussed in [19,20].

$$V_s = \frac{c}{\sqrt{\epsilon_r \mu_r}} \quad (1)$$

where,  $c$  is the speed of light,  $\epsilon_r$  the relative permittivity, and  $\mu_r$  the relative permeability and it is 1 for non-magnetic materials.

### 3. Results and Discussion

The results for the characterisation techniques discussed in section 2.3 is presented here.

#### 3.1 XRD Pattern

Figure 3 shows the XRD diffraction patterns of PTFE and PTFE/SLS composites. It can be seen that pattern of the PTFE exhibits a high-pitched peak and five lowly-appearing peaks positioned at  $18.05^\circ$ ,  $31.53^\circ$ ,  $36.60^\circ$ ,  $37.13^\circ$ ,  $41.18^\circ$ , and  $49.07^\circ$ . The peaks correlate to the (100), (110), (200), (107), (108), and (210) planes and are identified with the ICSD index of PTFE (ICSD 00-047-2217) [21,22]. Also, it can be observed that the PTFE sharpest peak appears to shrink as the filler content increases. However, no unrelated peak was recorded in the composites, indicating only a pure physical interaction occurred between the PTFE and SLS filler[23].

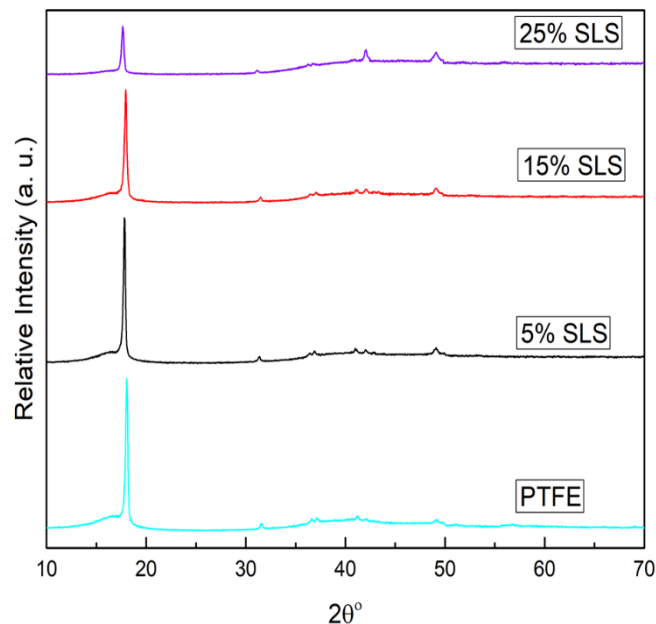


Fig. 3. XRD diffractograms of PTFE and PTFE/SLS composites

#### 3.2 Complex Permittivity

It can be observed in Figures 4, and 5 that, at lower SLS content, PTFE/SLS composites exhibited low values of the  $\epsilon'$  and  $\epsilon''$ , which increased considerably with more SLS filler content. This is expected as the addition of fillers with a higher dielectric constant than the matrix results in a high dielectric constant and loss factor of the composite and is consistent with previous works [21,24]. Further observation indicated that as the frequency changes from 1 GHz to 12 GHz, the  $\epsilon'$  and  $\epsilon''$  decreased, which is attributed to dipole-dipole relaxation [25–27]. At 5 wt.%, 10 wt.%, 15 wt.%, 20 wt.%, and 25 wt.% SLS filler content, the composite exhibited a dielectric constant of 2.11, 2.23, 2.35, 2.47, and 2.57, which decreased to 2.10, 2.22, 2.134, 2.46, and 2.56, respectively. The composites on the other hand showed a loss factor of 0.0023, 0.0025, 0.0027, 0.0029, and 0.0031 that decreased to 0.0022, 0.0024, 0.0026, 0.0029, 0.0030 at the 5 wt.%, 10 wt.%, 15 wt.%, 20 wt.%, and 25 wt.% of the filler content, respectively. However, the loss tangent, being a calculated parameter, followed the profile of the loss factor as shown in Figure 6. In addition, the variation of dielectric constant and loss factor with SLS filler content at some specific frequencies are depicted in Figures 7 and 8, while the corresponding empirical equations and the regression coefficients obtained from the graphs are presented in Tables 1 and 2, respectively.

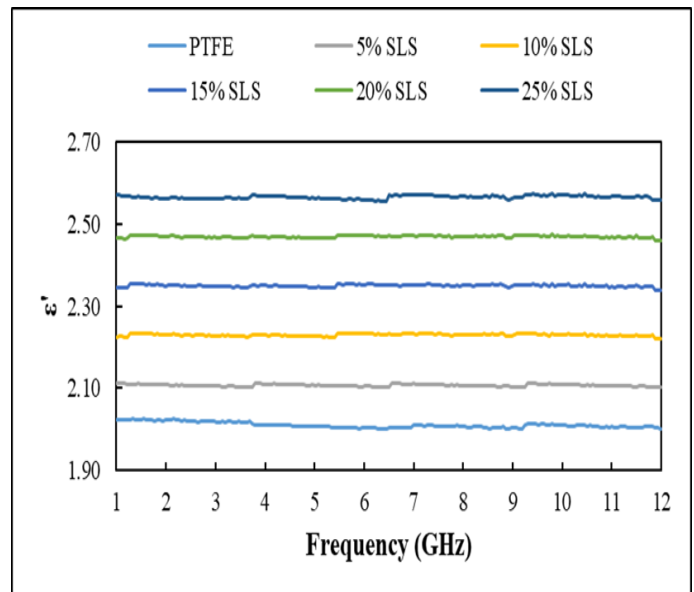


Fig. 4. Variation of relative permittivity with frequency and SLS filler content

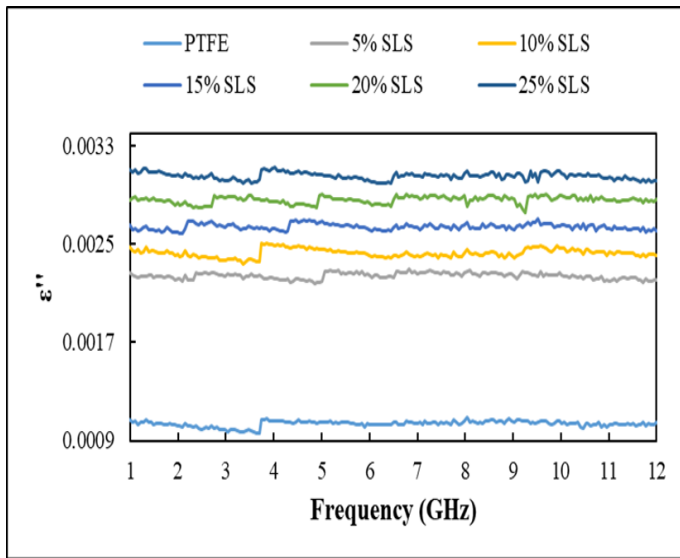


Fig. 5. Variation of loss factor with frequency and SLS filler content

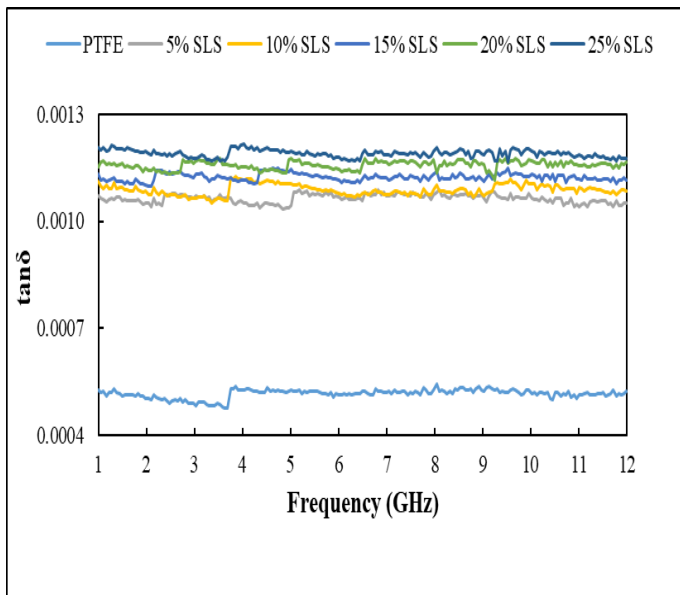


Fig. 6. Variation of loss tangent with frequency and SLS filler content

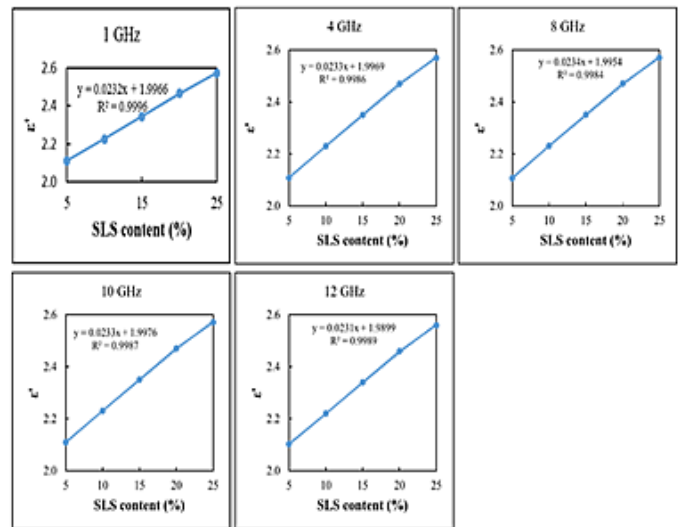


Fig. 7. Variation of relative permittivity with SLS filler content at specific frequencies

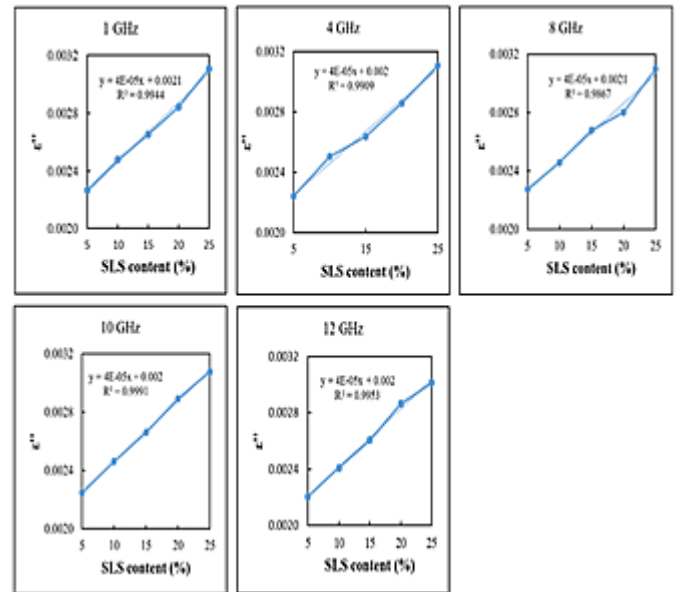


Fig. 8. Variation of loss factor with SLS filler content at specific frequencies

Table 1. Empirical equations and regression coefficient at specified frequencies for dielectric constant

Frequency (GHz)	Equation	Regression Coefficient ( $R^2$ )
1.0	$\epsilon' = 0.0232x + 1.9966$	0.9996
4.0	$\epsilon' = 0.0233x + 1.9969$	0.9986
8.0	$\epsilon' = 0.0234x + 1.9954$	0.9984
10.0	$\epsilon' = 0.0233x + 1.9976$	0.9987
12.0	$\epsilon' = 0.0231x + 1.9899$	0.9989

Table 2. Empirical equations and regression coefficient at specified frequencies for loss factor

Frequency (GHz)	Equation	Regression Coefficient ( $R^2$ )
1.0	$\epsilon'' = 4E - 05 + 0.0021$	0.9944
4.0	$\epsilon'' = 4E - 05 + 0.0020$	0.9909
8.0	$\epsilon'' = 4E - 05 + 0.0021$	0.9867
10.0	$\epsilon'' = 4E - 05 + 0.0020$	0.9991
12.0	$\epsilon'' = 4E - 05 + 0.0020$	0.9953

As revealed in Table 1, the regression coefficient correlation was close to unity at all specified frequencies. This implies a strong correlation between the  $\epsilon'$  and the SLS filler content. Similarly, the  $\epsilon''$  of the PTFE/SLS composites, as depicted in Fig. 7, increased linearly with the SLS filler content, giving a regression correlation of  $R^2 > 0.98$  as highlighted by Table 2. This result indicates a robust correlation between the  $\epsilon''$  and SLS filler content. A similar pattern has been reported in [28]. Furthermore, Table 3 compared the dielectric properties achieved in this work with reported literature on PTFE-based composites characterised using other methods.

Table 3. Comparison of dielectric properties of ptfе/sls composite characterised using ocp technique with reported ptfе-based composites characterised via other methods

Filler	Method	Filler content (wt.%)	Freq. (GHz)	$\epsilon'$	$\tan\delta$	References
T-GF	Stripline resonance	8	10	2.31	0.0009	[4]
Al <sub>2</sub> O <sub>3</sub> -hBN/GFs	Stripline resonance	40	10	3.53	0.0022	[21]
Recycled SLS	RWG	10	10	2.28	0.0017	[29]
BST	Hakki-Coleman	50	10	16.00	0.0052	[7]
Al <sub>2</sub> Mo <sub>3</sub> O <sub>12</sub>	TE <sub>011</sub> mode	30	9-12	3.6	0.0018	[30]
SLS	OCP	10	10	2.23	0.0011	This work

### 3.3 Propagation Speed

The propagation speed and its variation with SLS filler content and frequency is depicted in Figure 9. It can be seen the  $V_s$  increases with the frequency. At 1 GHz, the PTFE/SLS composites exhibited a  $V_s$  of  $2.04 \times 10^8$  m/s,  $2.00 \times 10^8$  m/s,

$1.94 \times 10^8$  m/s,  $1.91 \times 10^8$  m/s, and  $1.88 \times 10^8$  m/s, which varied to  $2.06 \times 10^8$  m/s,  $2.03 \times 10^8$  m/s,  $1.95 \times 10^8$  m/s,  $1.94 \times 10^8$  m/s, and  $1.91 \times 10^8$  m/s at 12 GHz for 5 wt.%, 10 wt.%, 15 wt.%, 20 wt.%, and 25 wt.% filler contents, respectively. The increased propagation speed was due to the lower values of relative permittivity at higher frequencies.

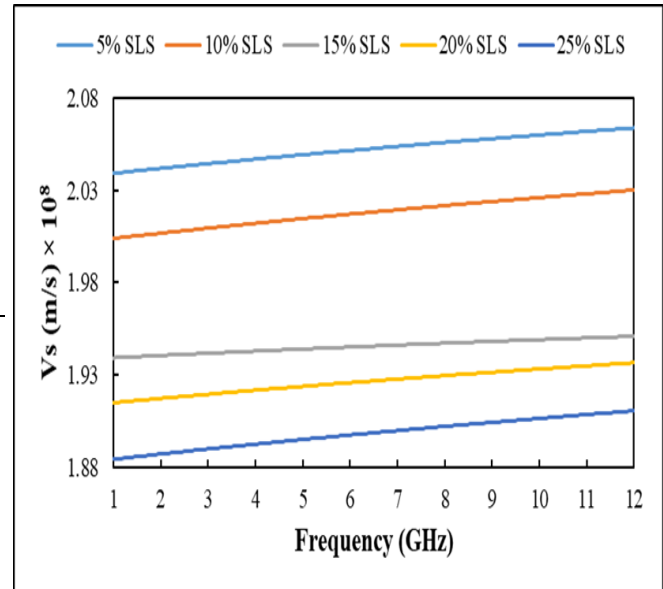


Fig. 9. Variation of propagation speed with SLS filler content and frequency

### 4. Conclusion

PTFE/SLS composites with different SLS content were prepared and fabricated using the dry powder mixing method. The dielectric characterisation was performed using the simple OCP technique at microwave frequency range of 1 GHz to 12 GHz. XRD diffractogram confirmed the phase of the PTFE and physical nature of the interaction between PTFE and SLS Phases. The values of the  $\epsilon'$  and  $\epsilon''$ , and  $\tan\delta$  were found to have increased with SLS filler content and decreased with frequency, consistent with previous studies. Also  $\epsilon'$  and  $\epsilon''$  were discovered to have a linear related with SLS filler content, thereby, achieving a  $R^2 > 0.98$ . In addition, the propagation speed was found to increase with frequency and decrease with SLS filler content. Furthermore, the optimum filler loading with balanced dielectric properties was obtained at 10 wt.% with the value of  $\epsilon'$ ,  $\epsilon''$ ,  $\tan\delta$ , and  $V_s$  of 2.23, 0.0022, 0.0011, and  $2.06 \times 10^8$  m/s. Thus, the OCP method can effectively characterised solid dielectric method for microwave substrate application.

### Acknowledgements

We are grateful to the Department of Physics, Faculty of Science, Universiti Putra Malaysia, for providing a conducive environment, materials and characterisation equipment to carry out this research.

## REFERENCES

- [1] Y. Tan, Y. Liu, X. Yan, G. Lu, K. Xie, J. Tong, and F. Meng, "Functionalized Al<sub>2</sub>O<sub>3</sub> fillers/glass fibers cloth/PTFE composites with excellent thermal properties," *J. Mater. Sci. Mater. Electron.* **33**, 8815–8821 (Springer US, 2022).
- [2] X. Cai, X. Dong, W. Lv, C. Ji, Z. Jiang, X. Zhang, T. Gao, K. Yue, and X. Zhang, "Synergistic enhancement of thermal conductivity for low dielectric constant boron nitride–polytetrafluoroethylene composites by adding small content of graphene nanosheets," *Compos. Commun.* **17**, 163–169 (Elsevier Ltd, 2020).
- [3] M. D. Zahidul Islam, Y. Fu, H. Deb, M. D. Khalid Hasan, Y. Dong, and S. Shi, "Polymer-based low dielectric constant and loss materials for high-speed communication network: Dielectric constants and challenges," *Eur. Polym. J.* **200**, 112543 (Elsevier Ltd, 2023).
- [4] Q. Li, P. Liu, K. Mahmood, N. Zhang, and Y. Che, "Improved properties of PTFE composites filled with glass fiber modified by sol–gel method," *J. Mater. Sci. Mater. Electron.* **32**, 23090–23102 (Springer US, 2021).
- [5] H. Wang, F. Zhou, J. Guo, H. Yang, J. Tong, and Q. Zhang, "Modified BCZN particles filled PTFE composites with high dielectric constant and low loss for microwave substrate applications," *Ceram. Int.* **46**, 7531–7540 (Elsevier Ltd and Techna Group S.r.l., 2020).
- [6] K. Zhang, D. Zhao, W. Chen, L. Zheng, L. Yao, Y. Qiu, and F. Xu, "Three-dimensional woven structural glass fiber/polytetrafluoroethylene (PTFE) composite antenna with superb integrity and electromagnetic performance," *Compos. Struct.* **281**, 115096 (Elsevier Ltd, 2022).
- [7] P. Jiang and J. Bian, "Low dielectric loss BST/PTFE composites for microwave applications," *Int. J. Appl. Ceram. Technol.* **16**, 152–159 (2019).
- [8] Z. Hu, X. Liu, T. Ren, H. A. M. Saeed, Q. Wang, X. Cui, K. Huai, S. Huang, Y. Xia, et al., "Research progress of low dielectric constant polymer materials," *J. Polym. Eng.* **42**, 677–687 (2022).
- [9] H. Wang, F. Zhou, J. Guo, H. Yang, J. Tong, and Q. Zhang, "Modified BCZN particles filled PTFE composites with high dielectric constant and low loss for microwave substrate applications," *Ceram. Int.* **46**, 7531–7540 (Elsevier Ltd and Techna Group S.r.l., 2020).
- [10] K. P. Murali, S. Rajesh, O. Prakash, A. R. Kulkarni, and R. Ratheesh, "Preparation and properties of silica filled PTFE flexible laminates for microwave circuit applications," *Compos. Part A Appl. Sci. Manuf.* **40**, 1179–1185 (Elsevier Ltd, 2009).
- [11] J. Wang, E. G. Lim, M. P. Leach, Z. Wang, and K. L. Man, "Open-ended coaxial cable selection for measurement of liquid dielectric properties via the reflection method," *Math. Probl. Eng.* **2020** (2020).
- [12] C. L. Brace and S. Etoz, "An analysis of open-ended coaxial probe sensitivity to heterogeneous media," *Sensors (Switzerland)* **20**, 1–13 (2020).
- [13] A. Yakubu, Z. Abbas, N. Ibrahim, and A. Fahad, "The Effect of ZnO nanoparticles Filler on Complex Permittivity of ZnO-PCL Nanocomposite at Microwave Frequency," *Phys. Sci. Int. J.* **6**, 196–202 (2015).
- [14] C. Aydinalp, S. Joof, I. Dilman, I. Akduman, and T. Yilmaz, "Characterization of Open-Ended Coaxial Probe Sensing Depth with Respect to Aperture Size for Dielectric Property," *Sensors* **22**, 1–13 (2022).
- [15] A. Kundu and B. Gupta, "Broadband dielectric properties measurement of some vegetables and fruits using open ended coaxial probe technique," in *Int. Conf. Control. Instrumentation, Energy Commun. CIEC 2014*, (2014).
- [16] A. La Gioia, E. Porter, I. Merunka, A. Shahzad, S. Salahuddin, M. Jones, and M. O'Halloran, "Open-Ended Coaxial Probe Technique for Dielectric Measurement of Biological Tissues: Challenges and Common Practices," *Diagnostics* **8**, 40 (2018).
- [17] N. I. Sheen and I. M. Woodhead, "An open-ended coaxial probe for broad-band permittivity measurement of agricultural products," *J. Agric. Eng. Res.* **74**, 193–202 (1999).
- [18] M. Venkatesh, "Integrated Dual Frequency Permittivity Analyser using Cavity Perturbation Concept" ((Unpublished doctoral thesis). McGill University, 2002).
- [19] M. T. Sebastian, R. Uvic, and H. Jantunen, Eds., *Microwave Materilas and Applications*, in *Microw. Mater. Appl.* (John Wiley & Sons, Ltd, New Jersey, 2017).
- [20] I. A. Alhaji, Z. Abbas, M. H. Mohd Zaid, and A. M. Khamis, "Effects of Particle Size on the Dielectric , Mechanical , and Thermal Properties of Recycled Borosilicate Glass-Filled PTFE Microwave Substrates," *Polymers (Basel)*. **13**, 15 (2021).
- [21] Y. Tan, X. Yan, C. Tang, G. Lu, K. Xie, J. Tong, and F. Meng, "Dielectric and thermal properties of GFs/PTFE composites with hybrid fillers of Al<sub>2</sub>O<sub>3</sub> and hBN for microwave substrate applications," *J. Mater. Sci. Mater. Electron.*, 23325–23332 (Springer US, 2021).
- [22] W. Feng, L. Yin, Y. Han, J. Wang, K. Xiao, and J. Li, "Tribological and physical properties of PTFE-NBR self-lubricating composites under water lubrication," *Ind. Lubr. Tribol.* **73**, 82–87 (2021).
- [23] E. E. Mensah, Z. Abbas, R. S. Azis, N. A. Ibrahim, A. M. Khamis, and D. M. Abdalhadi, "Complex permittivity and power loss characteristics of  $\alpha$ -Fe<sub>2</sub>O<sub>3</sub>/polycaprolactone (PCL) nanocomposites: effect of recycled  $\alpha$ -Fe<sub>2</sub>O<sub>3</sub> nanofiller," *Heliyon* **6**, e05595 (Elsevier Ltd, 2020).
- [24] F. T. S. Gladson, R. Ramesh, and C. Kavitha, "Experimental investigation of mechanical, tribological and dielectric properties of alumina nano wire-reinforced PEEK/PTFE composites," *Mater. Res. Express* **6** (IOP Publishing, 2019).
- [25] A. D. Meli, Z. Abbas, M. H. Mohd Zaid, and N. A. Ibrahim, "The effects of SLS on structural and complex

- permittivity of SLS-HDPE composites,” *Adv. Polym. Technol.* **2019** (2019).
- [26] O. Boiko, D. Drozdenko, and P. Minárik, “Dielectric properties, polarization process, and charge transport in granular  $(\text{FeCoZr})_x(\text{Pb}(\text{ZrTi})\text{O}_3)_{(100-x)}$  nanocomposites near the percolation threshold,” *AIP Adv.* **12** (AIP Publishing, LLC, 2022).
- [27] G. Yang, J. Cui, Y. Ohki, D. Wang, Y. Li, and K. Tao, “Dielectric and relaxation properties of composites of epoxy resin and hyperbranched-polyester-treated nanosilica,” *RSC Adv.* **8**, 30669–30677 (Royal Society of Chemistry, 2018).
- [28] A. M. Khamis, Z. Abbas, A. F. Ahmad, R. S. Azis, D. M. Abdalhadi, and E. E. Mensah, “Experimental and computational study on epoxy resin reinforced with micro-sized OPEFB using rectangular waveguide and finite element method,” *IET Microwaves, Antennas Propag.* **14**, 752–758 (2020).
- [29] I. A. Alhaji, Z. Abbas, N. Zainuddin, N. A. Ibrahim, A. M. Khamis, and I. I. Lakin, “Recycled soda lime silica glass inclusion in polytetrafluoroethylene matrix as reinforcement for microwave substrate application,” *Mater. Sci. Eng. Technol.* **53**, 1373–1385 (2022).
- [30] J. Ren, P. Yang, Z. Peng, and X. Fu, “Novel  $\text{Al}_2\text{Mo}_3\text{O}_{12}$ -PTFE composites for microwave dielectric substrates,” *Ceram. Int.* **47**, 20867–20874 (Elsevier Ltd, 2021).